Available online at www.sciencedirect.com

SciVerse ScienceDirect

Ceramics International 38 (2012) 4501–4510

CERAMICS INTERNATIONAL

www.elsevier.com/locate/ceramint

Prediction compressive strength of lightweight geopolymers by ANFIS

Ali Nazari *, Gholamreza Khalaj

Department of Materials Science and Engineering, Saveh Branch, Islamic Azad University, Saveh, Iran

Received 5 February 2012; received in revised form 7 February 2012; accepted 8 February 2012
Available online 17 February 2012

Abstract

In the present work, compressive strength of lightweight inorganic polymers (geopolymers) produced by fine fly ash and rice husk bark ash together with palm oil clinker (POC) aggregates has been investigated experimentally and modeled based on adaptive network-based fuzzy inference systems (ANFIS). Different specimens made from a mixture of fine fly ash and rice husk bark ash with and without POC were subjected to compressive strength tests at 2, 7 and 28 days of curing. The specimens were oven cured for 36 h at 80 °C and then cured at room temperature until 2, 7 and 28 days. Addition of POC to the geopolymeric mixtures caused reduced strength at all ages of curing. However a considerable increase in strength to weight ratio was acquired for the specimen with a high content of fine POC particles at 28 days of curing. To build the ANFIS model, training, validating and testing were conducted using experimental results from 144 specimens. The used data in the ANFIS models were arranged in a format of six input parameters that cover the quantity of fine POC particles, the quantity of coarse POC particles, the quantity of FA + RHBA mixture, the ratio of alkali activator to ashes mixture, the age of curing and the test trial number. According to these input parameters, in the ANFIS models, the compressive strength of each specimen was predicted. The training, validating and testing results in the model have shown a strong potential for predicting the compressive strength of the geopolymer specimens in the considered range.

Keywords: Geopolymer; Compressive strength; Fly ash; Rice husk bark ash; Palm oil clinker; ANFIS

1. Introduction

Geopolymer materials have attracted a lot of attention for various applications due to their excellent fire resistance, low density, low cost, easy processing, environmentally friendly nature and excellent thermal properties [1].

The compressive strength of an inorganic polymer depends on both the ratio of Si/Al and the types of the utilized raw material. Fly ash (FA) and is recently used as a source material to produce geopolymer because of its suitable chemical composition along with favorable size and shape [2,3]. Fly ash is a solid, fine-grained material resulting from the combustion of pulverized coal in power station furnaces. The material is collected in mechanical or electrostatic separators. The term fly ash is not applied to the residue extracted from the bottom of boilers. Fly ashes capable of reacting with $Ca(OH)_2$ at room temperature can act as pozzolanic materials. Their pozzolanic activity is attributable to the presence of SiO_2 and Al_2O_3 in amorphous form. Fly ashes are particularly rich in SiO_2, Al_2O_3 and Fe_2O_3, and also contain other oxides such as CaO, MgO, MnO, TiO_2, Na_2O, K_2O, SO_3, etc. Fly Ash with a high content of CaO (15–40%) may be regarded as potentially hydraulic and capable of causing unsoundness in mortars and concrete [4].

Rice husk-bark ash (RHBA) is a solid waste generated by biomass power plants using rice husk and eucalyptus bark as fuel. The power plant company providing RHBA for this research reported that about 450 tons/day of RHBA are produced and discarded. The major chemical constituent of RHBA is SiO_2 (about 75%) [5,6]. Therefore, blending FA and RHBA can adjust the ratio of Si/Al as required.

In the previous work [7], the properties of geopolymeric specimens with FA, RHBA and palm oil clinker aggregates (POC), a by-product in the incineration of Palm Oil Shell, to produce lightweight geopolymers was studied. POC is a light solid fibrous material which when crushed has the potential to be used as aggregate in lightweight concrete. The density and the strength of POC fall within the requirements of the structural lightweight concrete. This is anticipated to grow further with the global increase in vegetable oil demand. However, it is also the main contributor to the nation's pollution

* Corresponding author. Tel.: +98 255 2241511.
E-mail address: alinazari84@aut.ac.ir (A. Nazari).

0272-8842/$36.00
doi:10.1016/j.ceramint.2012.02.026

problem, which includes the annual production of 2.6 million tonnes of solid waste in the form of oil palm shells [8]. In this work, the compressive strength of geopolymers with these materials as aggregates has been modeled by adaptive network-based fuzzy inference systems (ANFIS).

Several works have addressed utilizing of computer-aided prediction of engineering properties including those done by the authors [9–12]. Adaptive network-based fuzzy inference systems (ANFIS) is the famous hybrid neuro-fuzzy network for modeling the complex systems [13]. ANFIS incorporates the human-like reasoning style of fuzzy systems through the use of fuzzy sets and a linguistic model consisting of a set of IF-THEN fuzzy rules. The main strength of ANFIS models is that they are universal approximators [13] with the ability to solicit interpretable IF-THEN rules. Nowadays, the artificial intelligence-based techniques like ANFIS [14] have been successfully applied in the engineering applications. However, there is a lack of investigations on metallurgical aspects of materials.

As authors' knowledge, there are no works on utilizing a mixture of FA, RHBA and POC to produce lightweight geopolymers except the previous work [7]. In addition, since the concept of geopolymers is rather new and there are few works on their properties, application of computer programs like ANFIS to predict their properties is rarely reported. The aim of this study is to presenting suitable model based on ANFIS to predict the compressive strength of lightweight geopolymers. Fine FA and RHBA were mixed by different amount of POC and subjected to compressive strength tests. As indicated in the previous work [7], the advantage of using a mixture of ashes is to control the SiO_2/Al_2O_3 ratio to achieve a suitable combination of waste materials result in higher strengths. Properties of the produced specimens were investigated after specific times of curing. Totally 144 data of compressive strength tests in different conditions were collected, trained, validated and tested by means of ANFIS. The obtained results have been compared by experimental ones to evaluate the software power for predicting the compressive strength of the geopolymer specimens.

2. Experimental procedure

The cementitious materials used in this work were FA and RHBA. Their chemical composition has been illustrated in Table 1. In addition, Fig. 1 shows SEM micrograph of the cementitious materials, respectively. The as-received ashes were sieved and the particles passing the finesses of 33 μm were grinded using Los Angeles mill 180 min. The average particle size obtained for FA was 3 μm with the BET specific surface of 38.9 m^2/g. The average particle size obtained for RHBA was 7 μm with the BET specific surface of 33.1 m^2/g. Fig. 2 shows the particle size distribution of the two produced samples. As mentioned in the previous work [7], both FA and RHBA are amorphous and hence reactive.

Table 1
Chemical composition of FA, RHBA and WG (wt%).

Material	SiO_2	Al_2O_3	Fe_2O_3	CaO	SO_3	Na_2O	Loss on ignition
FA	35.21	23.23	12.36	20.01	2.36	0.36	0.24
RHBA	81.36	0.4	0.12	3.23	0.85	–	3.55
WG	34.21	–	–	–	–	13.11	–

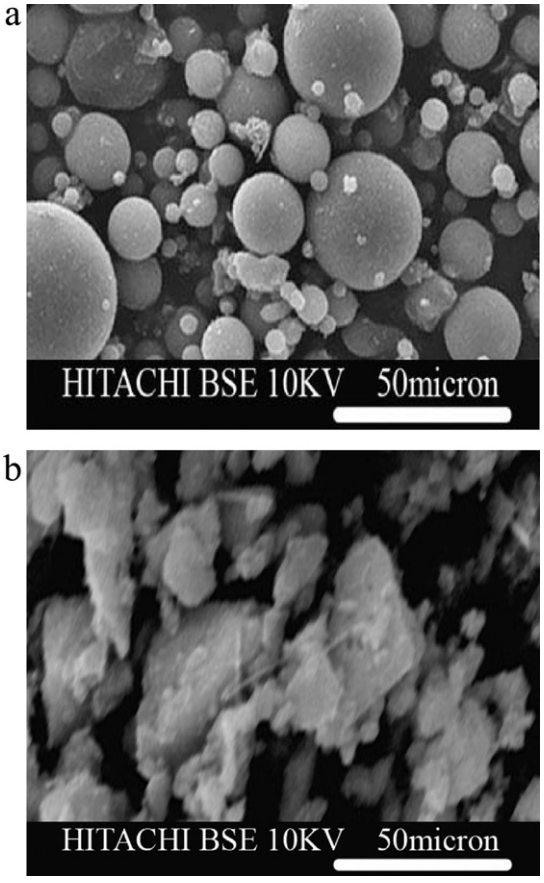

Fig. 1. SEM micrograph of (a) FA and (b) RHBA used in this study [7].

POC particles less than 7 mm and 7–18 mm size were used as fine and coarse aggregate. The density of fine and coarse POC was 1015 and 693 kg/m^3 respectively.

Sodium silicate solution or water glass (WG) and sodium hydroxide (NaOH) were used as the solution part of the mixture. WG was used without following modification, but the sodium hydroxide was diluted to different concentrations before using. The chemical composition of the utilized WG is also given in Table 1.

Totally 2 series of geopolymer specimens each contain different mixture of FA, RHBA and POC as illustrated in Table 2 were prepared for compressive strength tests. The mixture of FA to RHBA had a constant ratio of 70:30 and a bulk density of 2318 kg/m^3 to achieve SiO_2/Al_2O_3 ratio equals to approximately 3 [7]. The mixed alkali activator of sodium silicate solution and sodium hydroxide was used. Sodium hydroxide was diluted by tap water to have concentrations of 12 M since this concentration was found to produce the best strength [7]. The solution was left under ambient conditions until the excess heat had completely dissipated to avoid accelerating the setting of the geopolymeric specimens. The sodium silicate solution was mixed with the sodium hydroxide solution. The ratio of the

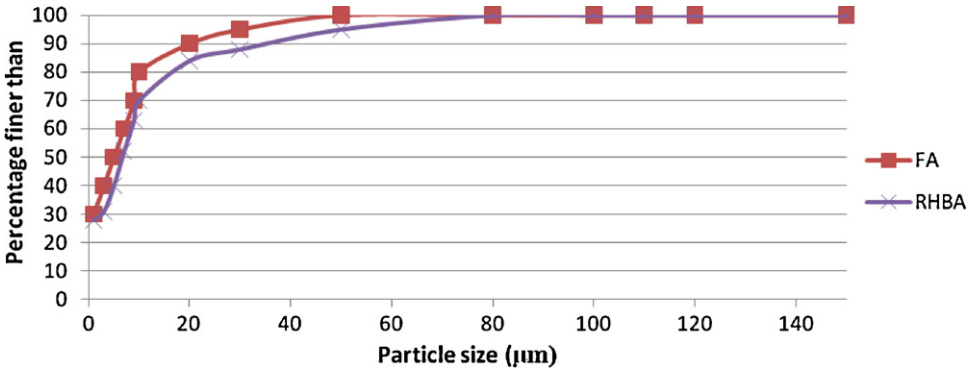

Fig. 2. Particle size distribution pattern of the different ashes used in this study.

sodium silicate solution to sodium hydroxide solution was 2.5 in accordance to the previous work [7]. For all samples, the mass ratio of alkali activator to FA-RHBA mixture was 0.4. Pastes were mixed by shaking for 5–10 min to give complete homogenisation. The mixtures were cast in ∅ 30 mm × 60 mm polypropylene cylinders. The mixing was done in an air-conditioned room at approximately 25 °C. The molds were half-filled, vibrated for 45 s, filled to the top, again vibrated for 45 s, and sealed with the lid. The mixtures were then precured for 24 h at room temperature. Precuring time before application of heat induces significant dissolution of silica and alumina from fly ash and formation of a continuous matrix phase, increasing, therefore, the homogeneity of the geopolymeric materials [15]. After the precuring process, the samples and molds were placed in a water bath to prevent moisture loss and the carbonation of the surface. The batches were put in the oven at the elevated temperatures of 80 °C for 36 h. Again this temperature and time was found to have the best effect on compressive strength of the specimens [7]. The compressive strength results of the produced specimens were measured on the cylindrical samples at 2, 7 and 28 days of curing (including oven curing). Three tests were carried out on each mixture and the average strength values were reported.

3. Experimental results and discussion

The compressive strength of the produced specimens has been illustrated in Fig. 3a–c for 2, 7 and 28 days of curing, respectively. On the whole, samples made with the fine RHBA and FA particles (C0 series) have shown considerably higher strength than the other series. This may be due to production of more compacted specimens in presence of finer FA and RHBA particles rather than POC particles. Fine particles are capable to fill the vacancies and produce more densified specimens which make them stronger to the applied loads. This has been confirmed in some works done on concrete specimens [16], but as the authors' knowledge, there are no reports which confirm this matter in geopolymers.

Fig. 3a–c shows that in the POC-contained specimens (i.e. all specimens except C0 series) the best strength has been achieved for fPOC70 specimens in all age of curing. Synthesized products are known to be very sensitive to

Table 2
Mixture proportioning of the utilized FA, RHBA and POC to produce geopolymeric specimens.

Sample designation	Volume fraction of fine + coarse POC in geopolymeric specimens (%)	The content of fine POC (kg/m^3)	The content of coarse POC (kg/m^3)	The content of FA (kg/m^3)	The content of RHBA (kg/m^3)	Density of the specimen (kg/m^3)
C0 (control)	0	0	0	2318	927.2	2318.0
fPOC30-1	5	15.2	24.3	2202.1	880.8	2248.0
fPOC30-2	10	30.5	48.5	2086.2	834.5	2178.0
fPOC30-3	20	60.9	97.0	1854.4	741.8	2038.1
fPOC30-4	40	121.8	194.0	1390.8	556.3	1758.2
fPOC30-5	50	152.3	242.6	1159.0	463.6	1618.2
fPOC50-1	5	25.4	17.3	2202.1	880.8	2244.8
fPOC50-2	10	50.8	34.7	2086.2	834.5	2171.6
fPOC50-3	20	101.5	69.3	1854.4	741.8	2025.2
fPOC50-4	40	203.0	138.6	1390.8	556.3	1732.4
fPOC50-5	50	253.8	173.3	1159.0	463.6	1586.0
fPOC70-1	5	35.5	10.4	2202.1	880.8	2241.6
fPOC70-2	10	71.1	20.8	2086.2	834.5	2165.2
fPOC70-3	20	142.1	41.6	1854.4	741.8	2012.3
fPOC70-4	40	284.2	83.2	1390.8	556.3	1724.3
fPOC70-5	50	355.3	104.0	1159.0	463.6	1573.0

Ashes mixture contains 70 wt% FA and 30 wt% RHBA.
Alkali activator (WG + NaOH) wt% to FA-RHBA wt% mixture ratio is 0.4.

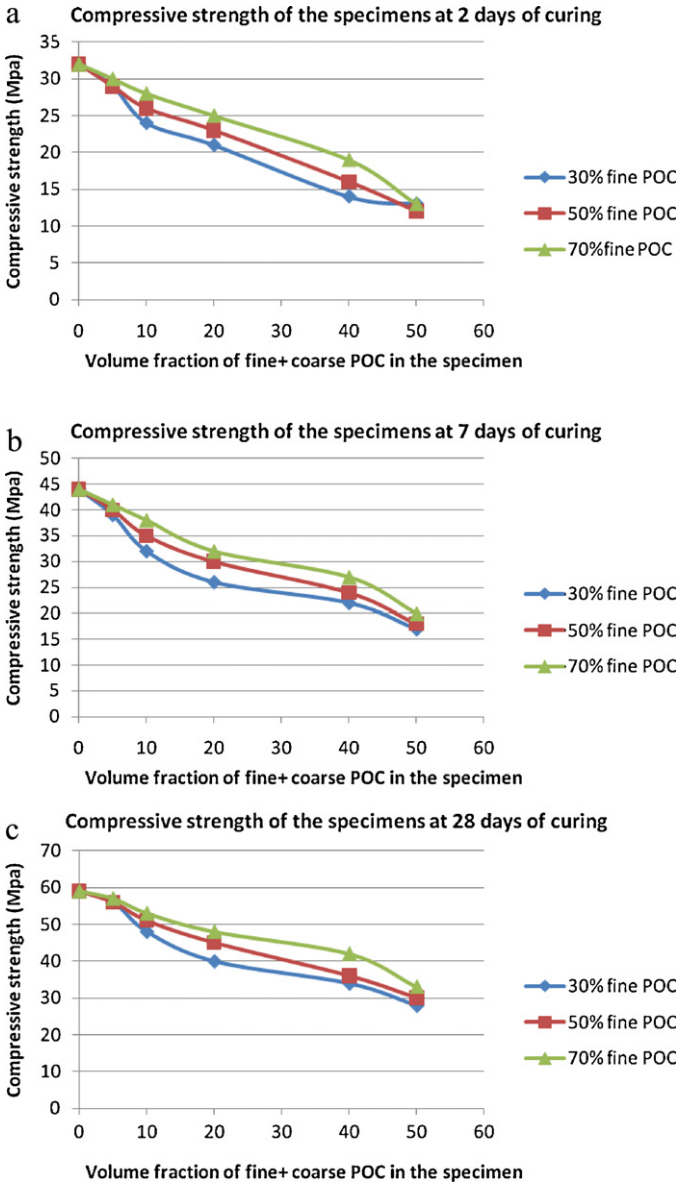

Fig. 3. The compressive strength of different geopolymeric specimens at (a) 2, (b) 7 and (c) 28 days of curing.

experimental conditions [17]. In the present work, the ashes mixture is constant and hence do not affect on the differences acquired by the test, solely. The differences between the achieved strengths may be due to two main factors. The first is that the reduction of ashes mixtures in POC-contained specimens reduces the final aluminosilicate and hence reduces the compressive strength in all ages of curing. The second reason is that the POC particles probably do not react with the alkali activator solution and therefore, the interface between POC particles and produced aluminosilicate is weak enough to be a suitable site for crack nucleation under compressive tension. On the other hand, the un-reacted POC particles decrease the homogeneity of the geopolymeric paste and hence reduce the final strength. The other reason for decreasing the compressive strength of POC-contained specimens with respect to POC-free specimens may be due to the lower strength of POC particles with respect to the formed aluminosilicate.

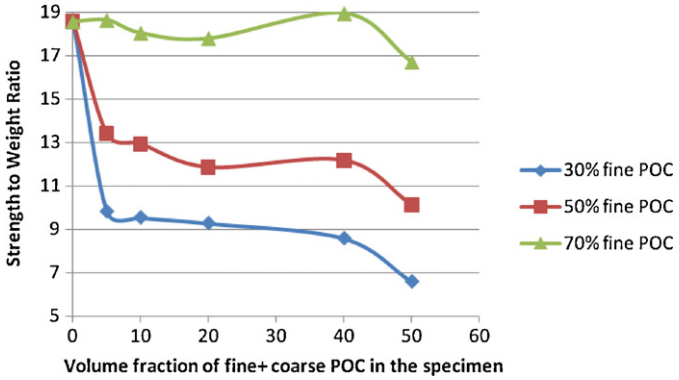

Fig. 4. 28 days strength to weight ratio of the geopolymeric specimens.

The best point of view for using POC particles is its low density with respect to the ashes mixture. Fig. 4 shows the 28 days strength to weight ratio (S/W) for all geopolymeric specimens. It is observed that for the specimens with 30% fine POC, POC particles negatively impact the S/W ratio of the specimens. This is more evident when the POC particles become more than 40%. For the specimens containing 50% fine POC, a partial increase in the S/W ratio is seen by increasing the POC content from 20% to 40%. However, after that, again S/W ratio is decreased. The best result of S/W ratio has been achieved by the specimens containing 70% fine POC particles. It is obvious that the specimens with POC content of 5% and 40% have an S/W ratio more than C0 series specimens. Since fPOC70-1 specimen has a low content of POC, the final decrease in compressive strength of the specimen is low and therefore, a slightly higher S/W ratio with respect to C0 series specimen is achieved. On the other hand, fPOC-4 specimen with a high content of fine POC particles has an acceptable compressive strength results in high S/W ratio. More than 40% POC reduces the S/W ratio as a result of the much reduced compressive strength. On the whole, high content fine POC particles could maintain the S/W ratio acceptable for the application in which the weight is a key factor for design.

4. Architecture of ANFIS

The architecture of an ANFIS model with two input variables is shown in Fig. 5. Suppose that the rule base of ANFIS contains two fuzzy IF-THEN rules of Takagi and Sugeno's type as follows:

Rule 1: IF x is A_1 and y is B_1, THEN $f_1 = p_1x + q_1y + r_1$.
Rule 2: IF x is A_2 and y is B_2, THEN $f_2 = p_2x + q_2y + r_2$.

In Fig. 5 fuzzy reasoning is illustrated and also the corresponding equivalent ANFIS architecture is shown in Fig. 6. The functions of each layer are described as follows [13,14,17,18]:

Layer 1 – Every node i in this layer is a square node with a node function:

$$O_i^1 = \mu_{A_i}(x) \tag{1}$$

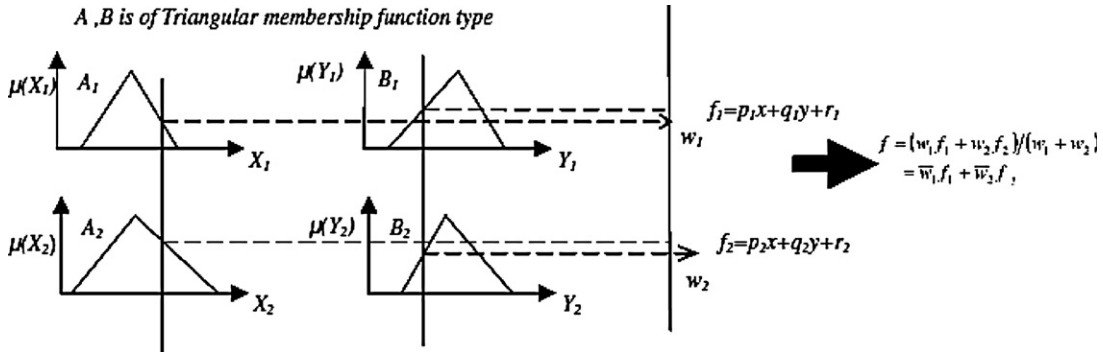

Fig. 5. The reasoning scheme of ANFIS [14].

where x is the input to node i, and A_i is the linguistic label (fuzzy sets: small, large, ...) associated with this node function.

Layer 2 – Every node in this layer is a circle node labeled P which multiplies the incoming signals and sends the product out. For instance,

$$W_i = \mu_{A_i}(y) \times \mu_{B_i}(y), \quad i = 1, 2 \tag{2}$$

Each node output represents the firing weight of a rule.

Layer 3 – Every node in this layer is a circle node labeled N. The ith node calculates the ratio of the ith rule's firing weight to the sum of all rule's firing weights:

$$W_i = \frac{W_i}{(W_1/W_2)}, \quad i = 1, 2 \tag{3}$$

Layer 4 – Every node in this layer is a square node with a node function:

$$O_i^4 = \bar{w}_i(p_i x + q_i y + r_1) \tag{4}$$

where $\bar{w}_i$ is the output of layer 3, and $\{p_i, q_i, r_i\}$ is the parameter set.

Layer 5 – The signal node in this layer is a circle node labeled R that computes the overall output as the summation of all incoming signals, i.e.,

$$O_i^5 = \sum_i \bar{w}_i f_i = \frac{\sum_i w_i f_i}{\sum_i w_i} \tag{5}$$

The basic learning rule of ANFIS is the back-propagation gradient descent, which calculates error signals recursively from the output layer backward to the input nodes. This learning rule is exactly the same as the back-propagation learning rule used in the common feed-forward neural networks [19,20]. Recently, ANFIS adopted a rapid learning method named as hybrid-learning method which utilizes the gradient descent and the least-squares method to find a feasible set of antecedent and consequent parameters [19,20]. Thus in this paper, the later method is used for constructing the proposed models.

4.1. ANFIS model structure and parameters

The structure of proposed ANFIS networks was consisted of six input variables including the quantity of fine POC particles (fP), the quantity of coarse POC particles (cP), the quantity of FA + RHBA mixture (A), the ratio of alkali activator to ashes mixture (A/A), the age of curing (C) and the test trial number (T). The value for output layer was compressive strength (f_S). The input space is decomposed by three fuzzy labels. In this paper, for comparison purposes, two types of membership functions (MFs) including the triangular (ANFIS-I) and Gaussian (ANFIS-II) were utilized to construct the suggested models. From the total 144 experimental data, the ANFIS models were trained by 102 randomly selected input-target pairs, validated by 21 and tested by the remained 21 data from testing pairs. Moreover, up to 1000 epochs were specified for training process to assure the gaining of the minimum error tolerance.

In this study the Matlab ANFIS toolbox is used for ANFIS applications. To overcome optimization difficulty, a program has been developed in Matlab which handles the trial and

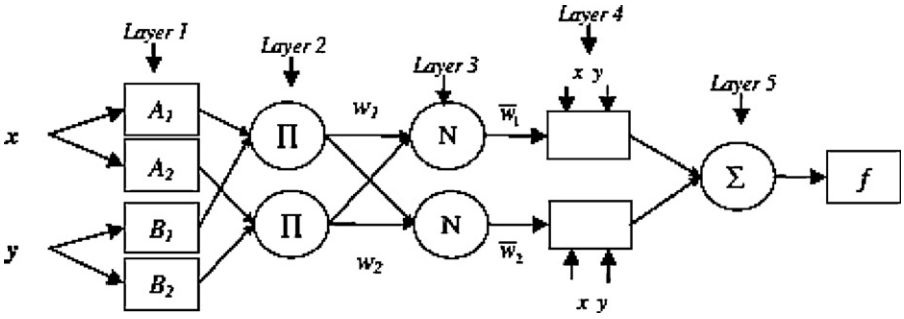

Fig. 6. Schematic of ANFIS architecture [14].

error process automatically [21–24]. The program tries various functions and when the highest RMSE (Root Mean Squared Error) of the testing set, as the training of the testing set is achieved, it was reported [21–24].

The IF-THEN rules in this study were achieved as follows. Suppose that the rule base of ANFIS contains two fuzzy IF-THEN rules of Takagi and Sugeno's type:

Rule 1: IF fP is A_1, cP is B_1, A is C_1, A/A is D_1, C is E_1 and T is F_1 THEN $f_1 = p_1fP + q_1cP + r_1A + s_1A/A + t_1C + u_1T + v_1$.

Rule 2: IF fP is A_2, cP is B_2, A is C_2, A/A is D_2, C is E_2 and T is F_2 THEN $f_2 = p_2fP + q_2cP + r_2A + s_2A/A + t_2C + u_2T + v_2$.

The corresponding equivalent ANFIS architecture is shown in Fig. 7. The functions of each layer are described as follows:

Layer 1 – Every node i in this layer is a square node with a node function:

$$O_i^1 = \mu_{A_i}(fP) \quad i = 1,2 \tag{6}$$

$$O_i^1 = \mu_{B_i}(cP) \quad i = 1,2 \tag{7}$$

$$O_i^1 = \mu_{C_i}(A) \quad i = 1,2 \tag{8}$$

$$O_i^1 = \mu_{D_i}\left(\frac{A}{A}\right) \quad i = 1,2 \tag{9}$$

$$O_i^1 = \mu_{E_i}(C) \quad i = 1,2 \tag{10}$$

$$O_i^1 = \mu_{F_i}(T) \quad i = 1,2 \tag{11}$$

where fP, cP, A, A/A, C and T are inputs to node i, and A_i, B_i, C_i, D_i, E_i and F_i are the linguistic label (fuzzy sets: small, large, ...) associated with this node function.

Layer 2 – Every node in this layer is a circle node labeled $\prod$ which multiplies the incoming signals and sends the product out. For instance,

$$W_i = \mu_{A_i}(fP) \times \mu_{B_i}(cP) \times \mu_{C_i}(A) \times \mu_{D_i}\left(\frac{A}{A}\right) \times \mu_{E_i}(C) \times \mu_{F_i}(T), \quad i = 1,2 \tag{12}$$

Each node output represents the firing weight of a rule.

Layer 3 – Every node in this layer is a circle node labeled N. The ith node calculates the ratio of the ith rule's firing weight to the sum of all rule's firing weights:

$$W_i = \frac{W_i}{(W_1/W_2)}, \quad i = 1,2 \tag{13}$$

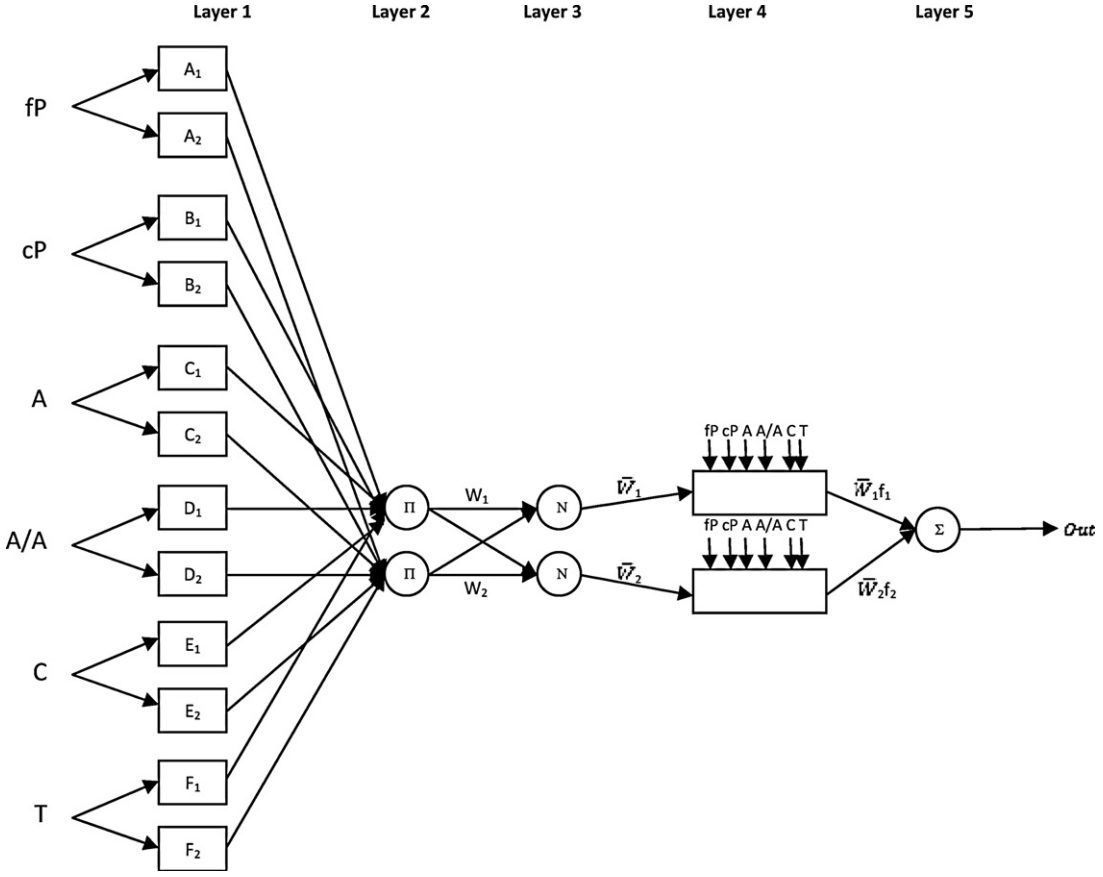

Fig. 7. Schematic of ANFIS architecture utilized in this work.

Table 3
Data sets for comparison of experimental results with tested and validated results predicted from ANFIS-I and ANFIS-II models.

The phase name	Number of set	The quantity of fine POC particles (fP) (kg/m^3)	The quantity of coarse POC particles (cP) (kg/m^3)	The quantity of FA + RHBA mixture (A) (kg/m^3)	The ratio of alkali activator to ashes mixture (A/A)	The age of curing (C) (day)	The test trial number (T)	Compressive strength values obtained from experiments (MPa)	Compressive strength values predicted by ANFIS-I model (MPa)
Validating	3	0	0	2318	927.2	2	3	34.8	36.3
	17	35.5	10.4	2202.1	880.8	2	2	31.8	30.1
	20	30.5	48.5	2086.2	834.5	2	2	25.2	24.4
	41	203	138.6	1390.8	556.3	2	2	15.7	15.5
	52	355.3	104	1159	463.6	2	1	12.1	14.4
	56	15.2	24.3	2202.1	880.8	7	2	40.2	39
	58	25.4	17.3	2202.1	880.8	7	1	41.2	38.2
	63	35.5	10.4	2202.1	880.8	7	3	43.9	42.5
	73	60.9	97	1854.4	741.8	7	1	24.4	26
	78	101.5	69.3	1854.4	741.8	7	3	30.9	31.2
	87	203	138.6	1390.8	556.3	7	3	24.5	23.9
	97	355.3	104	1159	463.6	7	1	18	19.1
	98	355.3	104	1159	463.6	7	2	21.8	17.7
	100	15.2	24.3	2202.1	880.8	28	1	51	51
	109	30.5	48.5	2086.2	834.5	28	1	46.1	45.8
	111	30.5	48.5	2086.2	834.5	28	3	48.5	49
	117	71.1	20.8	2086.2	834.5	28	3	56.2	55.7
	119	60.9	97	1854.4	741.8	28	2	40.4	39.8
	129	121.8	194	1390.8	556.3	28	3	35	33.3
	135	284.2	83.2	1390.8	556.3	28	3	44.6	45.7
	137	152.3	242.6	1159	463.6	28	2	28.3	26.5
Testing	2	0	0	2318	927.2	2	2	31.4	33.4
	8	0	0	2318	927.2	28	2	60.2	60.2
	16	35.5	10.4	2202.1	880.8	2	1	27.6	29.5
	22	50.8	34.7	2086.2	834.5	2	1	25.5	26.2
	23	50.8	34.7	2086.2	834.5	2	2	26	25.8
	29	60.9	97	1854.4	741.8	2	2	21.2	19.8
	48	152.3	242.6	1159	463.6	2	3	13.1	14.2
	50	253.8	173.3	1159	463.6	2	2	11.8	10.7
	53	355.3	104	1159	463.6	2	2	13.5	11.6
	60	25.4	17.3	2202.1	880.8	7	3	36.8	40.7
	64	30.5	48.5	2086.2	834.5	7	1	30.4	32.7
	81	142.1	41.6	1854.4	741.8	7	3	33.5	35.9
	84	121.8	194	1390.8	556.3	7	3	23.1	20.3
	89	284.2	83.2	1390.8	556.3	7	2	26.5	28.2
	94	253.8	173.3	1159	463.6	7	1	17.8	16.3
	95	253.8	173.3	1159	463.6	7	2	19.8	15.3
	102	15.2	24.3	2202.1	880.8	28	3	63.2	54.4
	105	25.4	17.3	2202.1	880.8	28	3	57.7	56
	113	50.8	34.7	2086.2	834.5	28	2	51	49.9
	126	142.1	41.6	1854.4	741.8	28	3	50.1	53.2
	133	284.2	83.2	1390.8	556.3	28	1	40.7	34

The phase name	Number of set	The quantity of fine POC particles (fP) (kg/m^3)	The quantity of coarse POC particles (cP) (kg/m^3)	The quantity of FA + RHBA mixture (A) (kg/m^3)	The ratio of alkali activator to ashes mixture (A/A)	The age of curing (C) (day)	The test trial number (T)	Compressive strength values obtained from experiments (MPa)	Compressive strength values predicted by ANFIS-II model (MPa)
Validating	1	0	0	2318	927.2	2	1	29.8	31.9
	5	0	0	2318	927.2	7	2	46.2	43.1
	14	25.4	17.3	2202.1	880.8	2	2	27.3	28.6
	16	35.5	10.4	2202.1	880.8	2	1	27.6	29.5
	19	30.5	48.5	2086.2	834.5	2	1	21.8	22.9
	22	50.8	34.7	2086.2	834.5	2	1	25.5	24.9
	29	60.9	97	1854.4	741.8	2	2	21.2	19.4
	48	152.3	242.6	1159	463.6	2	3	13.1	12
	51	253.8	173.3	1159	463.6	2	3	13.4	12
	52	355.3	104	1159	463.6	2	1	12.1	12.4

Table 3 (*Continued*)

The phase name	Number of set	The quantity of fine POC particles (fP) (kg/m^3)	The quantity of coarse POC particles (cP) (kg/m^3)	The quantity of FA + RHBA mixture (A) (kg/m^3)	The ratio of alkali activator to ashes mixture (A/A)	The age of curing (C) (day)	The test trial number (T)	Compressive strength values obtained from experiments (MPa)	Compressive strength values predicted by ANFIS-II model (MPa)
	53	355.3	104	1159	463.6	2	2	13.5	14.9
	62	35.5	10.4	2202.1	880.8	7	2	40.6	40.8
	69	50.8	34.7	2086.2	834.5	7	3	35.7	35.8
	84	121.8	194	1390.8	556.3	7	3	23.1	21.4
	85	203	138.6	1390.8	556.3	7	1	24	21.7
	86	203	138.6	1390.8	556.3	7	2	23.5	23.5
	101	15.2	24.3	2202.1	880.8	28	2	53.8	53.6
	104	25.4	17.3	2202.1	880.8	28	2	52.6	55
	121	101.5	69.3	1854.4	741.8	28	1	45.5	40.3
	122	101.5	69.3	1854.4	741.8	28	2	43.2	42.6
	136	152.3	242.6	1159	463.6	28	1	26.3	27.7
Testing	3	0	0	2318	927.2	2	3	34.8	32.1
	4	0	0	2318	927.2	7	1	39.6	42
	6	0	0	2318	927.2	7	3	46.2	42.2
	12	15.2	24.3	2202.1	880.8	2	3	32.8	28.1
	20	30.5	48.5	2086.2	834.5	2	2	25.2	23.7
	21	30.5	48.5	2086.2	834.5	2	3	25	24.4
	31	101.5	69.3	1854.4	741.8	2	1	23.2	21.6
	37	121.8	194	1390.8	556.3	2	1	12.6	15.2
	39	121.8	194	1390.8	556.3	2	3	14.7	15.8
	40	203	138.6	1390.8	556.3	2	1	16	15.4
	71	71.1	20.8	2086.2	834.5	7	2	36.9	38.2
	77	101.5	69.3	1854.4	741.8	7	2	28.8	29.8
	87	203	138.6	1390.8	556.3	7	3	24.5	23.3
	89	284.2	83.2	1390.8	556.3	7	2	26.5	28.1
	92	152.3	242.6	1159	463.6	7	2	17.7	20.9
	99	355.3	104	1159	463.6	7	3	20.2	21.7
	108	35.5	10.4	2202.1	880.8	28	3	58.2	57.2
	129	121.8	194	1390.8	556.3	28	3	35	36.3
	138	152.3	242.6	1159	463.6	28	3	29.4	27.9
	140	253.8	173.3	1159	463.6	28	2	28.8	28.1
	142	355.3	104	1159	463.6	28	1	30.9	37.4

Layer 4 – Every node in this layer is a square node with a node function:

$$O_i^4 = \bar{w}_i\left(P_i\,fP + q_i cP + r_i A + s_i\left(\frac{A}{A}\right) + t_i C + u_i T + v_i\right) \tag{14}$$

where $\bar{w}_i$ is the output of layer 3, and $\{p_i, q_i, r_i, s_i, t_i, u_i, v_i, z_i\}$ is the parameter set.

Layer 5 – The signal node in this layer is a circle node labeled R that computes the overall output as the summation of all incoming signals, i.e.,

$$O_i^5 = \sum_i \bar{w}_i f_i = \frac{\sum_i w_i f_i}{\sum_i w_i} \tag{15}$$

5. Predicted results and discussion

In this study, the error arose during the training, validating and testing in ANFIS-I and ANFIS-II models could be expressed as absolute fraction of variance (R^2) which are calculated by Eq. (16) [25]:

$$R^2 = 1\left(\frac{\sum_i (t_i - o_i)^2}{\sum_i (o_i)^2}\right) \tag{16}$$

where t is the target value and o is the output.

All of the results obtained from experimental studies and predicted by using the training, validating and testing results of ANFIS-I and ANFIS-II models are given in Fig. 8a and b, respectively. The linear least square fit line, its equation and the R^2 values have been shown in these figures for the training and testing data. Also, inputs values and experimental results with validating and testing results obtained from ANFIS-I and ANFIS-II models have been given in Table 3, respectively. As it is visible in Fig. 8, the values obtained from the training, validating and testing in ANFIS-I and ANFIS-II models are very close to the experimental results. The result of testing phase in Fig. 8 shows that the ANFIS-I and ANFIS-II models are capable of generalizing between input and output variables with reasonably good predictions.

The performance of the ANFIS-I and ANFIS-II models is shown in Fig. 8. The best value of R^2 is 99.11% for training set in the ANFIS-II model. The minimum values of R^2 are 94.43%

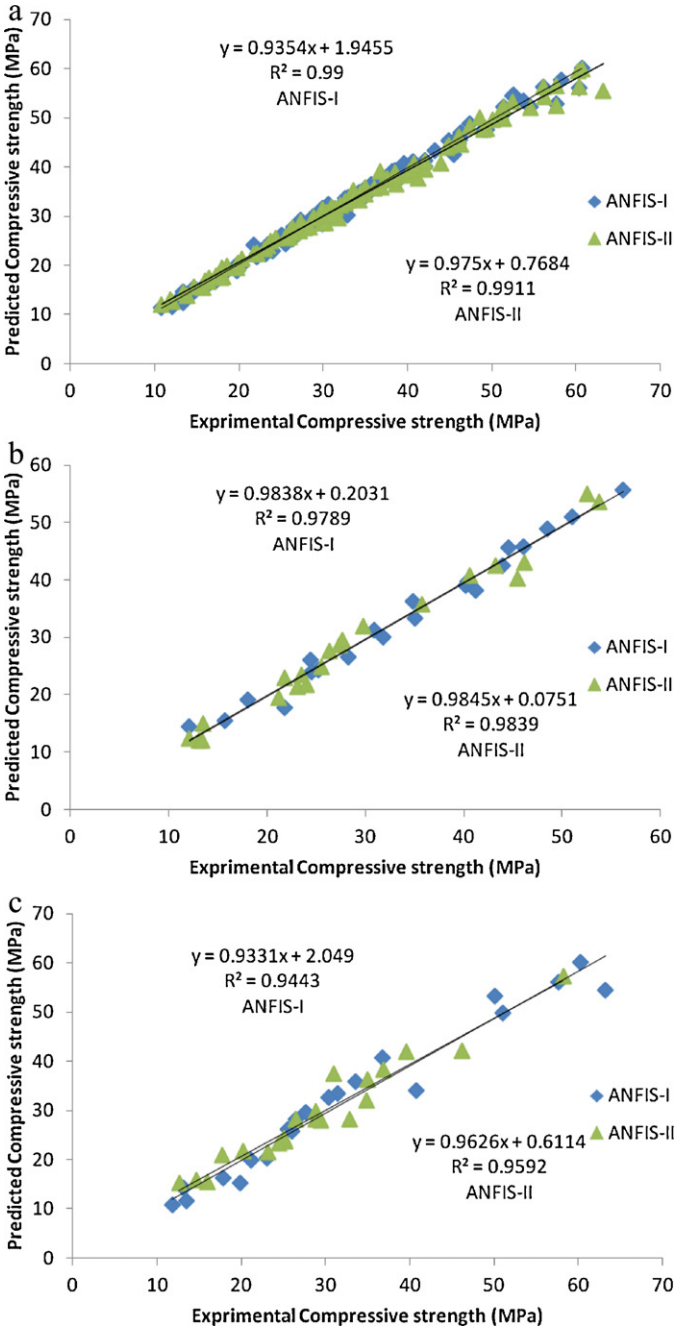

Fig. 8. The correlation of the measured and predicted compressive strength values of geopolymers in (a) training and (b) validating and (c) testing phase for ANFIS models.

for testing set in the ANFIS-I model. It seems that the superiority of ANFIS-II model is due to its suitable utilized function. All of R^2 values show that the proposed ANFIS-I and ANFIS-II models are suitable and can predict the compressive strength values very close to the experimental values.

6. Conclusions

1. Utilizing POC particles in the geopolymeric specimens reduces the final compressive strength at all ages of curing. However, using the finer POC particles results in a slightly stronger paste than the other POC-containing series.
2. The 28 days strength to weight ratio for the specimens with a high content of fine POC particles was higher than that of POC-free specimen which make it suitable for the applications in which the weight is a critical factor.
3. ANFIS can be an alternative approach for the evaluation of the effect of seeded mixture of FA and RHBA on compressive strength values of geopolymer specimens.
4. Comparison between ANFIS models in terms of R^2 showed that these models are capable to predict suitable results for compressive strength values of geopolymers.

References

[1] P. He, D. Jia, T. Lin, M. Wang, Y. Zhou, Effects of high-temperature heat treatment on the mechanical properties of unidirectional carbon fiber reinforced geopolymer composites, Ceram. Int. 36 (2010) 1447–1453.
[2] R.R. Lloyd, J.L. Provis, J.S.J. van Deventer, Microscopy and microanalysis of inorganic polymer cements. 1: remnant fly ash particles, J. Mater. Sci. 44 (2009) 608–619.
[3] S. Kumar, R. Kumar, S.P. Mehrotra, Influence of granulated blast furnace slag on the reaction, structure and properties of fly ash based geopolymer, J. Mater. Sci. 45 (2010) 607–615.
[4] E. Álvarez-Ayuso, X. Querol, F. Plan, A. Alastuey, N. Moreno, M. Izquierdo, O. Font, T. Moreno, S. Diez, E. Vázquez, M. Barra, Environmental, physical and structural characterisation of geopolymer matrixes synthesised from coal (co-)combustion fly ashes, J. Hazard. Mater. 154 (2008) 175–183.
[5] V. Sata, C. Jaturapitakkul, K. Kiattikomol, Influence of pozzolan from various byproduct materials on mechanical properties of high-strength concrete, Constr. Build. Mater. 21 (7) (2007) 1589–1598.
[6] W. Tangchirapat, R. Buranasing, C. Jaturapitakkul, P. Chindaprasirt, Influence of rice husk–bark ash on mechanical properties of concrete containing high amount of recycled aggregates, Constr. Build. Mater. 22 (8) (2008) 1812–1819.
[7] A. Nazari, S. Riahi, A. Bagheri, Designing water resistant lightweight geopolymers produced from waste materials, Mater. Des. 35 (2012) 296–302.
[8] B.S. Mohammed, M.A. Al-Ganad, M. Abdullahi, Analytical and experimental studies on composite slabs utilising palm oil, clinker concrete, Constr. Build. Mater. 25 (2011) 3550–3560.
[9] A. Nazari, S. Riahi, Computer-aided design of the effects of Fe_2O_3 nanoparticles on split tensile strength and water permeability of high strength concrete, Mater. Des. 32 (2011) 3966–3979.
[10] A. Nazari, A.A. Milani, M. Zakeri, Modeling ductile to brittle transition temperature of functionally graded steels by artificial neural networks, Comput. Mater. Sci. 50 (2011) 2028–2037.
[11] A. Nazari, A.A. Milani, Modeling ductile to brittle transition temperature of functionally graded steels by fuzzy logic, J. Mater. Sci. 46 (18) (2011) 6007–6017.
[12] A. Nazari, N. Didehvar, Analytical modeling impact resistance of aluminum–epoxy laminated composites, Compos. Part B 42 (2011) 1912–1919.
[13] J.S.R. Jang, ANFIS: adaptive-network-based fuzzy inference system, IEEE Trans. Syst. Man Cybern. 23 (3) (1993) 665–685.
[14] M. Sarıdemir, Predicting the compressive strength of mortars containing metakaolin by artificial neural networks and fuzzy logic, Adv. Eng. Soft 40 (9) (2009) 920–927.
[15] P. Chindaprasirt, T. Chareerat, V. Sirivivatnanon, Workability and strength of coarse high calcium fly ash geopolymer, Cem. Concr. Compos. 29 (2007) 224–229.
[16] A. Naji Givi, S. Abdul Rashid, A. Nora, F. Aziz, M.A. Mohd Salleh, Assessment of the effects of rice husk ash particle size on strength, water

permeability and workability of binary blended concrete, Constr. Build. Mater. 24 (11) (2010) 2145–2150.
[17] A.A. Ramezanianpour, M. Sobhani, J. Sobhani, Application of network based neuro-fuzzy system for prediction of the strength of high strength concrete, Amirkabir J. Sci. Technol. 5 (59-C) (2004) 78–93.
[18] A.A. Ramezanianpour, J. Sobhani, M. Sobhani, Application of an adaptive neurofuzzy system in the prediction of HPC compressive strength, in: Proceedings of the Fourth International Conference on Engineering Computational Technology, Civil-Comp Press, Lisbon, Portugal, 2004 p. 138.
[19] I.B. Topcu, M. Sarıdemir, Prediction of mechanical properties of recycled aggregate concretes containing silica fume using artificial neural networks and fuzzy logic, Comput. Mater. Sci. 42 (1) (2008) 74–82.
[20] J.S.R. Jang, C.T. Sun, Nuro-fuzzy modeling and control, Proc. IEEE 83 (3) (1995).
[21] I.H. Guzelbey, A. Cevik, A. Erklig, Prediction of web crippling strength of cold-formed steel sheetings using neural networks, J. Constr. Steel Res. 62 (2006) 962–973.
[22] I.H. Guzelbey, A. Cevik, M.T. Gögüs, Prediction of rotation capacity of wide flange beams using neural networks, J. Constr. Steel Res. 62 (2006) 950–961.
[23] A. Cevik, I.H. Guzelbey, Neural network modeling of strength enhancement for Cfrp confined concrete cylinders, Build. Environ. 43 (2008) 751–763.
[24] A. Cevik, I.H. Guzelbey, A soft computing based approach for the prediction of ultimate strength of metal plates in compression, Eng. Struct. 29 (3) (2007) 383–394.
[25] I.B. Topcu, M. Sarıdemir, Prediction of compressive strength of concrete containing fly ash using artificial neural network and fuzzy logic, Comput. Mater. Sci. 41 (3) (2008) 305–311.